Automated Segmentation of Cell Structure in Microscopy Images

Nicole Kerrison and Andy Bulpitt

School of Computing, University of Leeds, Woodhouse Lane, Leeds, LS2 9JT, U.K.

Keywords: Segmentation, Lighting Correction, Cell Motility, Microscopy, Lamellipodia, DIC.

Abstract: Understanding cell movement is important in helping to prevent and cure damage and disease. Increasingly, this study is performed by obtaining video footage of cells in vitro. However, as the number of images obtained for cellular analysis increases, so does the need for automated segmentation of these images, since this is difficult and time consuming to perform manually. We propose to automate the process of segmenting all parts of a cell visible in DIC microscopy video frames by providing an efficient method for correcting the lighting bias and a novel combination of techniques to detect different cell areas and isolate parts of the cell vital to their movement. To the best of our knowledge we contribute the only method able to automatically detect the thin cellular membranes in DIC images. We show that the method can be used to isolate features in order to detect variations vital to motility in differently affected cells.

1 INTRODUCTION

The study of cells is a key field in modern science in order to help understand biological processes. Currently, much of the analysis is conducted by hand but this can be time consuming and subject to human error. Automating this work would allow greater accuracy, with reproducible results at a higher speed. Automation would additionally allow for quantitative analysis of the data, rather than just qualitative.

The movement of cells is vital to many biological processes, as cells can move to infected areas or wounds which need healing, and abnormal cell movements can lead to disease and defects. In order to prevent and cure disease we need to be able to understand how cells migrate and morph, and to be able to measure their movement and change in shape (Dormann and Weijer, 2006; Zimmer et al., 2006).

This is particularly important in ameoboid cells, such as the myoblast cell, in which movement on substrate is achieved through a crawling motion. The cell extends large, but very thin protrusions called lamellipodia which stretch out and adhere to the substrate, providing anchor points for the cell to be pulled forward (Becker et al., 2000; Karp, 2010; Middleton and Sharp, 1984).

Biologists have taken videos of moving cells using time-lapse DIC (differential interference contrast) microscopy, in which the light beam is split with part passed through the cell and the difference calculated

to give a representation of the thickness of the cell, discussed further in Section 1.1. Due to the nature of DIC imaging, the thinly spread membranes of the lamellipodia are often barely visible, with the texture appearing the same as the background.

Researchers in cell motility wish to obtain information about the cells and their movement, both in unaffected (wildtype) cells, and in those in which genes have been affected (knocked down or over expressed) or chemicals added. One particular chemical, blebbistatin, is an inhibitor which has been found to affect the cells contractile forces and has an affect on the lamellipodia and the cells' motility (Limouze et al., 2004; Straight et al., 2003; Kolega, 2006). Researchers wish to know if brenk also has a similar affect on the lamellipodia, and therefore the cells' movement.

To find out more about the lamellipodia they need to be segmented separately from the cell in order to calculate information about their size and shape, and how these change over time. This work aims to segment not only the cell but also divide it into its component parts to enable this information to be calculated. This is done in a fully automated manner, in which a video can be analysed with no need for manual selection or segmentation, and no necessity for manual adjustment of parameters. We firstly present results confirming our general segmentation method works against a variety of DIC cell images, then focus on the particular application of lamellipodia segmenta-

tion within the biological domain.

1.1 DIC Microscopy

There have been many advances in light microscopy over the years, particularly the discovery of Green Fluorescent Protein (GFP) which fluoresces under blue light. As such it can be used to tag proteins or genes, enabling the detection and localisation of their expression (Tsien, 1998). However, the illumination can cause cell damage which affects both the movement and lifespan of a cell (Stephens and Allan, 2003).

Using transmitted light for imaging live cells can provide additional information and detail relating to the cell shape. One such method is phase contrast microscopy, which can outline the cells and highlight some organelles. This, however, surrounds the imaged cell by a bright halo making it difficult to identify distinct edges (Lane and Stebbings, 2006).

Another method is DIC microscopy, in which a beam splitter is applied to the light and half passed through the cell. By measuring the difference in the lengths of the optical paths the thickness of the cell can be estimated (Murphy, 2001). The resulting image appears as three-dimensional, and high contrast images can be created showing more detail than previous methods. This is particularly useful for transparent objects, which would normally be difficult to see without staining (Salmon and Tran, 2007; Schwartz et al., 2003).

Although the method of obtaining DIC images can provide many advantages, it can also cause problems when the images are to be processed. The images appear to be illuminated by a highly oblique light source, which creates a shadow and light 3D effect, but this also causes a large variation in the brightness of the background (Schwartz et al., 2003; Kuijper and Heise, 2008) and the object being studied, which can be seen in Figures 2(a) and 2(b).

2 RELATED WORK

When studying normal and abnormal cell movement it is not only important to find the location of the cell, but to segment it in such a way that the size and shape of the cell can also be recorded for analysis. Although a lot of previous work on cells has involved counting or tracking the cells, far less has been produced on shape analysis. Pincus and Theriot compared methods for cell shape analysis by investigating methods which provided interpretable and accurate numerical representations of the cell shape

(Pincus and Theriot, 2007). They found that principal component analysis was the method which can most accurately capture modes of shape variation, and this has been very successful on keratocyte cells, which can be modelled with only a few modes of shape variability (Keren et al., 2008). However, this approach is not suitable for amorphous structures such as myoblast cells where the features cannot be aligned.

Much of the previous work on cell shape analysis has involved manual segmentation, which is very time consuming. Wu et al. used a two step procedure to reduce this cost, by manually selecting each region of an image which contained a cell (Wu et al., 1995). They found that this reduced the variation in intensity levels which occurs across images and allowed for local thresholding. Further work to automate the process of segmentation has often been for the purposes of cell counting or tracking, in which obtaining the cell boundary is not necessary. Jiang et al. used SIFT to compare key-points and track cells in DIC videos, without the necessity to find cell boundaries (Jiang et al., 2010). Bise et al. also looked at tracking and intentionally excluded portions of the cells from the segmentation, such as the long thin parts which deform significantly as these can confuse the tracking (Bise et al., 2009).

Level sets have used to automate segmentation. This was found to be successful on cells which showed symmetry and did not contain too many visible sub-structures (Kuijper and Heise, 2008). Young and Gray also relied on similarly shaped elliptical cells applying a curvature constraint and segmenting cells using edge contours (Young and Gray, 1996). Segmentation of complex shaped cells was investigated by Simon et al. but the method was found to be unsuitable for images with a large background to cell ratio, and for cells with a thin membrane (Simon et al., 1998), such as ours. These cells (with poor intensity contrast) were excluded from the analysis.

Li and Kanade developed a method for preconditioning DIC images to assist with segmentation, but when tested on our images the areas of most contrast appear as if affected by a very bright "shadow" which distorts the cell shape and there is no increase in the definition of the thinner, less obvious parts of the cell (Li and Kanade, 2009), as can be seen in Figure 1(a). ImageJ (Abramoff et al., 2004) is an imaging program which provides a method (pseudo-flat-field) for intensity correction of images. When tested on our images using a smaller filter this produced a "glow" around the cell and slight blurring, as well as a small amount of "shadow" in one corner. As the size of the filter was increased, so did the area of shadow. The result of using the default size is shown in Figure 1(b).

(a) Original   (b) With colour   (c) Blurred background   (d) Corrected   (e) Corrected with colour
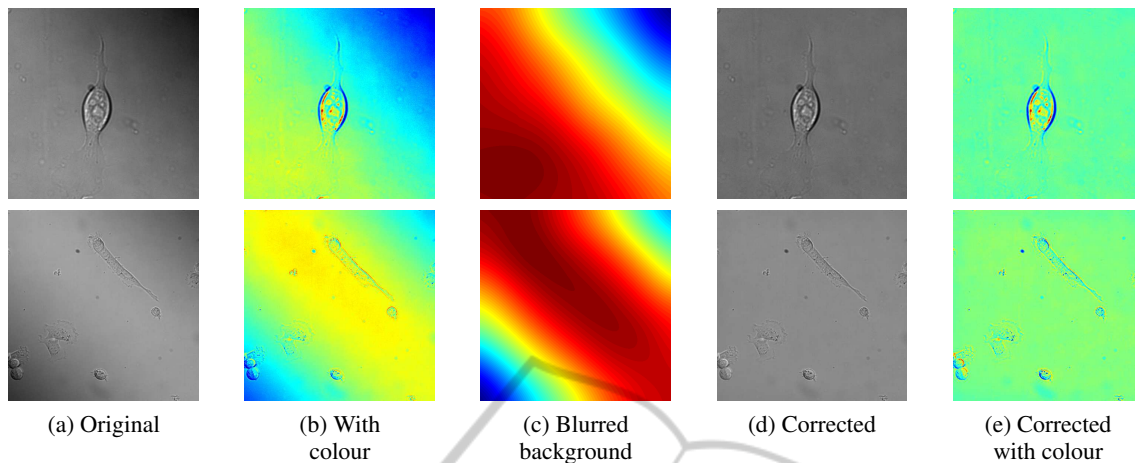
Figure 2: Correcting for DIC shadow effect.
The first column shows the original frames and the second shows these with colour applied, to make the lighting variation more visible. The middle column shows the brightness of pixels over the background when the cell is blurred out. The final two columns show the resulting images, with the shadow effect corrected.

(a) Preconditioned Image   (b) ImageJ Pseudo-Flatfield
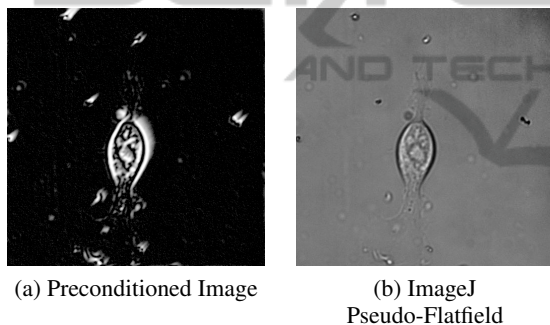
Figure 1: Alternative methods to account for lighting variations.
The first image shows the result of preconditioning the image using the method from (Li and Kanade, 2009). The second image uses ImageJ (Abramoff et al., 2004) to correct the intensity but using a filter large enough not to affect the cell results in a darker area still visible in the top right of the image.

3 LIGHTING CORRECTION

DIC imaging causes lighting variations across the frame, as can be seen in Figure 2(a). Two example frames are shown, with the lighting and shadow appearing differently in both. The top image appears to be lit from the bottom left, with shadow appearing in the top right, and the bottom image appears to be lit from roughly the middle with shadow appearing in two corners, Figure 2(a). A colour map has been added to the images, as in Figure 2(b), to make the light variations more visible to the eye. The lighting variations occur smoothly across the whole image, and affect the cells as well as the background.

Using a Gaussian blur, the cell detail can be re- moved, shown in Figure 2(c). The intensity differences between the original and the blurred image are stored for every pixel, which allows us to obtain the detail of the cell and other objects in the image, without need to model the background. The background is then set to the mean of the image intensity of the frame. The stored values are then re-added to the adjusted image to show the cell and other information with no loss of detail, as seen in Figure 2(d), and again in 2(e) with added colour to make the lack of variation more apparent. This is repeated for each frame in the video.

The pixel values were calculated across the diagonal with the greatest variation in intensity (e.g. bottom left to top right in the examples shown in Figure 2) before and after the background lighting variation was corrected. It can be seen from Figure 3 that this efficient method creates a uniform background level across the frames.

This was also tested on images from an internet search and was demonstrated to be equally effective on all DIC images tested, including those where the cells took up the majority of the frame. Some example results are shown in Figure 3. The first two rows are the images from Figure 2, the third is an online image of HeLa cells, in which there is very little background, and the fourth is an online image of a C. Elegans worm tail. The original images all show a variation in background lighting as well as the detail of the object being examined, as can be seen in Figure 3(a). The uneven background without the detail (after the Gaussian blur) is shown in 3(b). The corrected images all show a more even background illumination without loss of detail of the cell or worm, as seen in Figure

(a) Original
Image

(b) After
Gaussian
Blur

(c) Corrected
Image
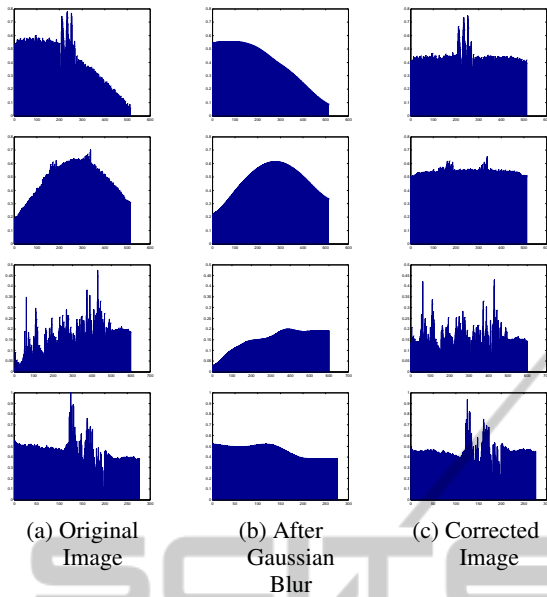
Figure 3: Pixel values before and after correction.
The pixel values were recorded along the diagonal with the most lighting variation before and after lighting correction. The first two images are those shown in Figure 2 and the second two were found using an online image search. All show a more even background without loss of information of the cell or worm.

3(c). This is successful even with only small amounts of background visible as the lighting variations occur not only over the background but also across the cells. Although other there are other methods for correcting lighting, this efficient method proved suitable for all DIC images tested.

4 THRESHOLDING AND EDGE DETECTION

Due to the lighting variations in DIC images, thresholding based on brightness is not normally possible, as can be seen Figures 4(b) and 4(c). Our lighting adjustment method not only corrects the background visually, but also provides the mean to which the background is adjusted on which thresholding can be based. The image seen in Figure 4(d) shows in white those pixels in the light-corrected image that are more than 10% brighter or darker than the mean value, with those that are nearest to the mean being set to black as background.

The brightest and darkest areas of the image such as the main body of the cell can be detected using thresholding. In most cases, cell videos are taken of one particular type of cell, and as such the main bodies are of reasonably similar sizes. This stage allows

(a) Original

(b) Threshold
at 50%

(c) Threshold
around mean

(d) Threshold after
lighting correction
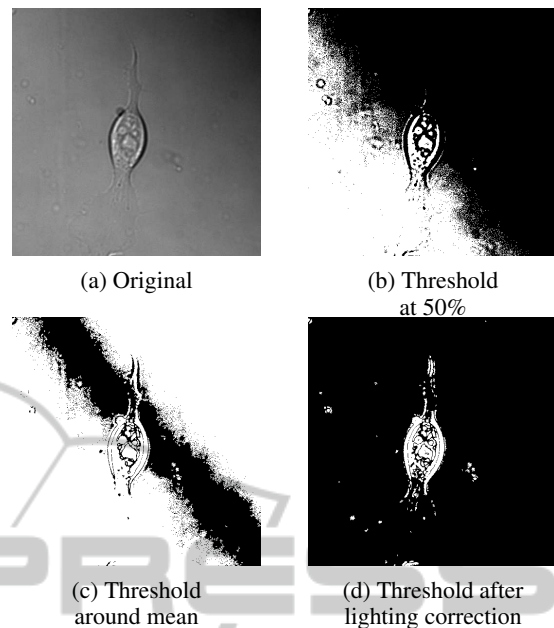
Figure 4: Thresholding DIC images.
Prior to lighting correction, it is not possible to segment DIC images using thresholding alone as the differences in the background cover the same intensities as the cell. The final image shows that the main parts of the cell can be easily thresholded after the lighting adjustment.

us to calculate the size and provides information for removing non-cellular material from the frame. Although this thresholding finds the main body of the cell, the fainter lamellipodium still needs to be segmented.

(a) Original

(b)
Threshold

(c)
Combined
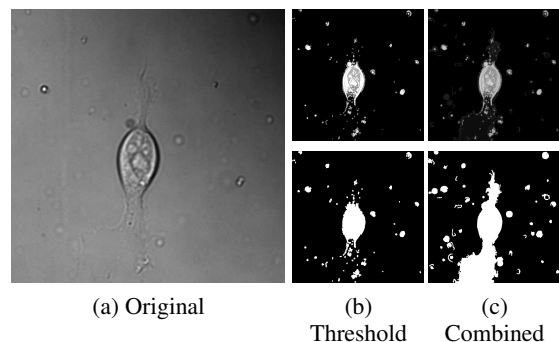
Figure 5: Combined results.
It can be seen that thresholding alone cannot detect large area of the lamellipodia at the bottom, but when combined with edge detection the full cell is detected. The images are also shown in binary beneath the results to aid viewing.

Taking $F(t)$ as a light corrected frame at time t, we apply a Canny Edge detection generating a set of edges $E(t)$. We only keep the subset of edges $e \subseteq E(t)$ which are connected to the "on" pixels in the thresholded image $F(t)$, as shown in Figure 5(c). The top

images are shown in greyscale, and the lower images are shown in binary with all non-zero pixels shown as white for clarity.

The resulting image is then filled, smoothed and the small non-cellular areas are removed, proportional to the body size calculated in the thresholding step. The result is a binary image in which the white areas are the cell and the black are the background. This white shape can be applied to the original image as a template to provide the boundary of the cell and to segment it from the background. We denote this cell segmentation at time t as $C(t)$.

| (a) Outline of | (b) Outline of | (c) Outline of |
| one cell | two cells | many cells |
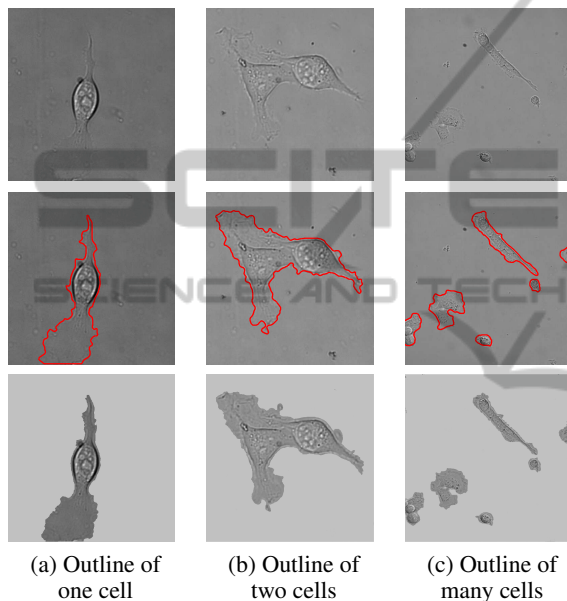
Figure 6: Outline of cells from the template.
Using the template created from the combined thresholding and edge detection method, the outline of the cells is traced onto the original image. As can be seen, the detection is very close to the actual edge, even when this is difficult to detect by eye. The bottom row of images have had the background manually adjusted so the outline of the cells can be seen.

The resulting segmentation is very close to the cell boundary (Figure 6), even where it is difficult to detect by eye. Manually adjusted images have been created to show the cells with a paler background to assist in visualisation. Additionally, it is shown to work on varying sizes of cells and with different degrees of background coverage. Tables 1 and 2 show the accuracy of the results which are discussed in section 7.1.

5 ITERATIVE CORRECTION

The resulting segmentation for the thresholding and edge detection method was very close to the man-

ual segmentation for most frames (which will be discussed in Section 7.1), but in some frames the lamellipodia were not entirely detected, an example of which can be seen in Figure 7(a). In these cases it was often also extremely difficult or even impossible to detect these areas by eye in the individual frame, but the location could be inferred from the movement in the surrounding frames. To detect these cases (of incomplete segmentation) the cell size was compared over consecutive frames, with those frames showing a significant increase or decrease being the most likely to not be entirely segmented.

We denote a cell segmentation at time t as $C(t)$. At each time-step, we compare the area of $C(t)$ with that of $C(t-1)$. If the area has changed by at least 10%, we take the intersection of $C(t-1)$ and $C(t+1)$ to generate the basis of a new segmentation image, $\hat{C}(t)$. As stated in section 4, we have a set of edges $E(t)$ generated from $F(t)$. We now keep those edges $\hat{e} \subseteq E(t)$ that are connected to $\hat{C}(t)$. We replace each segmentation $C(t)$ with the new version $\hat{C}(t) + \hat{e}$.

The entire process is then repeated over the entire video using the updated frames. This is run iteratively until such a time as no two consecutive frames have an area difference of greater than 10%, or until the method is creating no further changes, which is detected by comparing the list of sizes in consecutive runs.

The advantage of this iterative framework becomes evident where we have two or more consecutive erroneous segmentations. Take as an example the situation where $C(t)$ and $C(t+1)$ are incorrect; when taking the intersection of $C(t-1)$ and $C(t+1)$, we still obtain an incomplete representation of the cell. As such the initial pass of the method will not create a full segmentation throughout the video. However, if we repeat the full process as described above, segmentation improves at each pass until we converge on a more complete solution.

The resulting segmentation shows an improvement on the previous results, as shown in Figure 7(b), when compared with manually segmented cells (Tables 1 and 2).

6 SEGMENTATION OF LAMELLIPODIA

As previously discussed (Section 1), it is important to not only be able to segment the cell, but also to identify the component parts. As the size and spread of lamellipodia is vital to the cells movement, being able to calculate this can assist in learning about the cell's motility.

(a) Before Iterative
Correction

(b) After Iterative
Correction
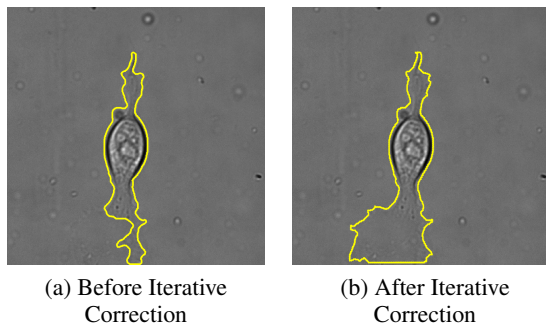
Figure 7: Correcting the Segmentation.
In some frames the lamellipodia is not fully segmented, as seen in (a). The previous and subsequent frames are used to correct this, as shown in (b). In this instance, the boundary from the segmentation is shown in yellow for clarity.

(a) Original
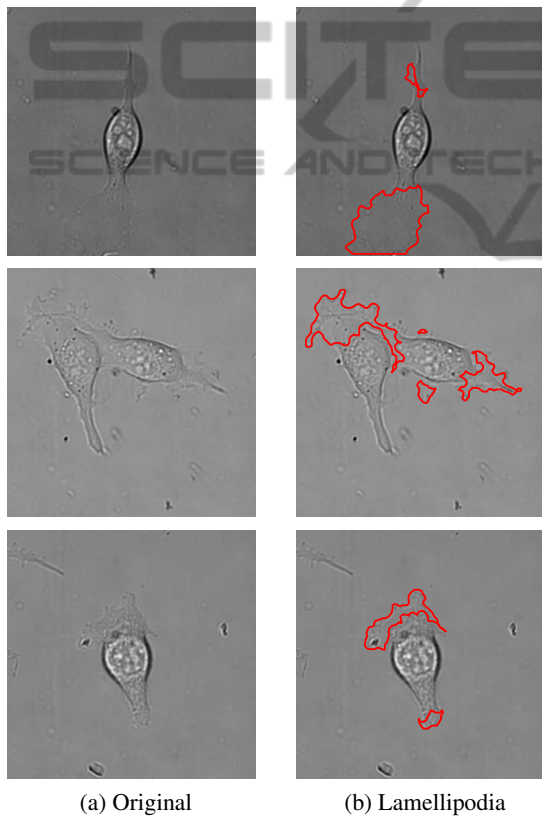
(b) Lamellipodia

Figure 8: Cells segmented to show lamellipodia.
The first columns show the original images, the second shows the segmented lamellipodia.

Figure 8 shows the lamellipodia being segmented separately from the cell body. As our method uses thresholding to find the main body of the cell this can be removed from the final segmentation to leave only the lamellipodia. From this, the size can be calculated over time and the individual regions tracked to assist in building a pattern of the growth.

The segmentation of the lamellipodia was applied to three groups of videos; those containing wildtype cells, those containing cells which had been affected by blebbistatin and those cells which had been affected by brenk. The size of the lamellipodia was calculated for each frame, as the absolute size and as relative to the size of the cell body to account for larger and smaller cells. This was used to assess the affect of these chemicals on the cells, and the results are discussed in Section 7.2.

7 RESULTS

The lighting correction method for preconditioning and the segmentation method were applied to all images from a variety of test sets with visually good results. The segmentation of the cell and the lamellipodia were then tested against a subgroup of 26 videos with the results for each shown below.

7.1 Results for Segmenting the Cell

Although the results for this system were obtained using a fully automated system, no other automated system could be found for comparison of results that was able to detect and segment the cells. The segmentation was instead compared to results using CellTrack (Sacan et al., 2008) by manually adjusting the parameters of the CellTrack algorithms to obtain the closest possible result to the cell boundary. The automated segmentations, both before and after the iterative correction, and the CellTrack segmentations were compared with manual segmentations using DICE (Table 1) and Jaccard (Table 2), which compare the overlap in segmentations. The average results are shown over each of three groups of videos; wildtype cells, those affected by the chemical blebbistatin and those affected by brenk.

Table 1: Comparison Of DICE Results (% accuracy).

	Wildtype	Blebb.	Brenk
Orig. Segmentation	89.75	86.64	89.33
After Correction	**90.13**	**87.35**	**90.95**
CellTrack	88.81	85.52	90.89

Table 2: Comparison Of Jaccard Results (% accuracy).

	Wildtype	Blebb.	Brenk
Orig. Segmentation	82.25	77.43	81.56
After Correction	**82.65**	**78.29**	**83.69**
CellTrack	80.20	75.49	83.44

The initial segmentation provided a very good result. From 910 frames tested, only 37 (roughly 4%)

had small parts of the lamellipodia missing. It can be seen that this still provides a better result than the best method involving manual adjustment in all but one case. After using the iterative correction method the resulting segmentation was more accurate in every case.

7.2 Results for Segmenting the Lamellipodia

The segmentation of the lamellipodia was also tested on wildtype cells, cells affected by blebbistatin and cells affected by brenk. Researchers wished to know if both the blebbistatin and the brenk had an effect on the lamellipodia, which would in turn affect the cells' motility, and if this affect was similar for both of them. Initially, the size was calculated for the lamellipodia in every frame as well as the size of the cell body.

It was found that the mean size-ratio was greater for both the brenk and blebbistatin (with an overall mean ratio of 0.40 and 0.39 respectively) compared to the wildtype cells (with a mean ratio of 0.18), as shown in Table 3. Whilst the mean size-ratio was larger in blebbistatin and brenk than in wildtype, we see comparatively more variation in wildtype size-ratios, as evidenced by a standard deviation of more than 0.24 relative to a mean of 0.18. Conversely, the spread of blebbistatin and brenk is smaller than the mean size-ratio in both cases. This could imply that although the lamellipodia is larger in both cases it does not have the same ability to change size by contracting and expanding as would be the case with wildtype cells.

Table 3: Size of Lamellipodia Comparative to Cell Body.

	Mean	Standard Deviation
Wildtype	0.1842	0.2448
Blebbistatin	0.4043	0.3337
Brenk	0.3923	0.3195

The size-ratios for every frame in each group of videos were compared with the Kolmogorov-Smirnov test against the null hypothesis that they were from the same distribution. Both the blebbistatin and the brenk were tested against the wildtype cells and in both cases were shown not to be from the same distribution (for wildtype and blebbistatin $p < 2.5 \times 10^{-18}$ and for wildtype and brenk $p < 8.5 \times 10^{-20}$). The blebbistatin and brenk when tested against each other, however, were not from different distributions ($p = 0.5227$).

8 CONCLUSIONS AND FURTHER WORK

We have proposed a method for segmenting cells in DIC images, even when there is very little contrast difference between the cell and the background. This involves a fast lighting correction technique which has proved successful on not only the cellular footage currently being assessed, but also on DIC images found online.

We provide a fully automated segmentation technique which can segment all parts of the cell including the thin membrane. To correct the images where the boundary does not fully encompass the lamellipodia we use an iterative method to improve the segmentation based on the surrounding frames. This is a fully automated system which provides a more accurate result than currently available tools which require manual input.

The results show that the cell can be accurately segmented, and the information gained in the process can then be used to identify lamellipodia separately. This allows us to obtain further information about the size of the components affecting the cells' movement. We have shown that when affected by brenk or blebbistatin the lamellipodia in cells grow differently to the lamellipodia in wildtype cells, and that overall the size is similar.

REFERENCES

Abramoff, M. D., Magelhaes, P. J., and Ram, S. J. (2004). Image processing with ImageJ. *Biophotonics Int*, 11(7):36–42.

Becker, W., Kleinsmith, L., and Hardin, J. (2000). *The world of the cell*. Benjamin/Cummings series in the life sciences. Benjamin Cummings.

Bise, R., Li, K., Eom, S., and Kanade, T. (2009). Reliably tracking partially overlapping neural stem cells in dic microscopy image sequences. In *MICCAI Workshop on Optical Tissue Image Analysis in Microscopy, Histopathology and Endoscopy (OPTMHisE)*, pages 67–77.

Dormann, D. and Weijer, C. J. (2006). Review: Imaging Of Cell Migration. *European Molecular Biology Organization Journal*, 25(15):3480 – 3493.

Jiang, R., Crookes, D., Luo, N., and Davidson, M. (2010). Live-Cell Tracking Using SIFT Features in DIC Microscopic Videos. *Biomedical Engineering, IEEE Transactions on*, 57(9):2219–2228.

Karp, G. (2010). *Cell Biology*. John Wiley and Sons, Asia, sixth edition.

Keren, K., Pincus, Z., Allen, G., Barnhart, E., Marriott, G., Mogilner, A., and Theriot, J. (2008). Mecha-

nism of shape determination in motile cells. *Nature*, 453(7194):475–480.

Kolega, J. (2006). The Role of Myosin II Motor Activity in Distributing Myosin Asymmetrically and Coupling Protrusive Activity to Cell Translocation. *Molecular Biology of the Cell*, 17(10):4435–4445.

Kuijper, A. and Heise, B. (2008). An automatic cell segmentation method for differential interference contrast microscopy. In *ICPR 2008. 19th International Conference on Pattern Recognition*, pages 1–4. IEEE.

Lane, J. D. and Stebbings, H. (2006). Transmitted light imaging. In Stephens, D., editor, *Cell Imaging*, Methods Express. Scion, Bloxham, Oxfordshire.

Li, K. and Kanade, T. (2009). Nonnegative mixed-norm preconditioning for microscopy image segmentation. In *Proceedings of the 21st Biennial International Conference on Information Processing in Medical Imaging (IPMI)*, pages 362–373.

Limouze, J., Straight, A. F., Mitchison, T., and Sellers, J. R. (2004). Specificity of blebbistatin, an inhibitor of myosin II. *Journal of muscle research and cell motility*, 25(4-5):337–341.

Middleton, C. and Sharp, J. (1984). *Cell Locomotion in Vitro: Techniques and Observations*. Croom Helm Ltd, Kent.

Murphy, D. B. (2001). *Fundamentals of Light Microscopy and Electronic Imaging*, chapter Differential Interference Contrast (DIC) Microscopy and Modulation Contrast Microscopy, pages 153 – 172. Wiley-Liss, New York, New York.

Pincus, Z. and Theriot, J. A. (2007). Comparison of quantitative methods for cell-shape analysis. *Journal of Microscopy*, 227(2):140–156.

Sacan, A., Ferhatosmanoglu, H., and Coskun, H. (2008). Celltrack: an open-source software for cell tracking and motility analysis. *Bioinformatics*, (14):1647–1649.

Salmon, E. D. and Tran, P. (2007). High-Resolution Video-Enhanced Differential Interference Contrast Light Microscopy. In Sluder, G. and Wolf, D. E., editors, *Digital Microscopy*, volume 81 of *Methods in Cell Biology*, pages 335 – 363. Academic Press, San Diego, California, third edition.

Schwartz, S., Murphy, D., Spring, K., and Davidson, M. (2003). de sénarmont bias retardation in dic microscopy. http://www.microscopyu.com/pdfs/DICMicroscopy.pdf. Nikon MicroscopyU.

Simon, I., Pound, C. R., Partin, A. W., Clemens, J. Q., and Christens-Barry, W. A. (1998). Automated image analysis system for detecting boundaries of live prostate cancer cells. *Cytometry*, 31(4):287–294.

Stephens, D. J. and Allan, V. J. (2003). Light Microscopy Techniques for Live Cell Imaging. *Science*, 300:82 – 86.

Straight, A. F., Cheung, A., Limouze, J., Chen, I., Westwood, N. J., Sellers, J. R., and Mitchison, T. J. (2003). Dissecting Temporal and Spatial Control of Cytokinesis with a Myosin II Inhibitor. *Science*, 299(5613):1743–1747.

Tsien, R. Y. (1998). The Green Fluorescent Protein. *Annual Review of Biochemistry*, 67:509 – 44.

Wu, K., Gauthier, D., and Levine, M. D. (1995). Live cell image segmentation. *Biomedical Engineering, IEEE Transactions on*, 42(1):1–12.

Young, D. and Gray, A. J. (1996). Cell identification in Differential Interference Contrast microscope images using edge detection. pages 66.1–66.10. 7th British Machine Vision Conference, BMVA Press.

Zimmer, C., Zhang, B., Dufour, A., Thebaud, A., Berlemont, S., Meas-Yedid, V., and Marin, J.-C. (2006). On the digital trail of mobile cells. *Signal Processing Magazine, IEEE*, 23(3):54 –62.